Supporting Information

High-efficient Overall Water Splitting Over Porous Interconnected Network by Nickel Cobalt Oxysulfide Interfacial Assembled Cu@Cu_2S Nanowires

*Duy Thanh Tran,[a] Van Hien Hoa,[a] Huu Tuan Le,[a] Nam Hoon Kim,[a] Joong Hee Lee[a,b]**

[a]Advanced Materials Institute for BIN Convergence Technology (BK21 Plus Global Program), Department of BIN Convergence Technology, Jeonbuk National University, Jeonju, Jeonbuk 54896, Republic of Korea.

[b]Carbon Composite Research Center, Department of Polymer-Nanoscience and Technology, Jeonbuk National University, Jeonju, Jeonbuk 54896, Republic of Korea

*Corresponding authors: E-Mail: jhl@jbnu.ac.kr (Joong Hee Lee)

Fax: +82 832702341; Tel: +82 832702342

Preparation of Cu@Cu_2S NWs network

For preparing Cu@Cu_2S NWs, a working electrode of the Cu NWs on 3DF (1 cm x 1 cm) was dippded in an an aqueous solution (50 mL) containing 0.75 M of thiourea, while Ag/AgCl and graphite rod were used as reference and counter electrode, respectively. An electrodeposition process was conducted at an applied potential of -1.0 V (*vs.* Ag/AgCl) for 100 s. After that, the sample was cleaned with water three times and was dried at 60 ^oC in a vacuum oven.

Preparation of Cu@Cu_2S@$NiO_{1-x}S_x$ NWs (or Cu@Cu_2S@$CoO_{1-x}S_x$ NWs) network

A piece of the Cu NWs on 3DF (1 cm x 1 cm), used as the working electrode, was dippded in an electrochemical cell containing 50 mL of water dispersed with 10 mM of $Ni(NO_3)_2$ (or

$Co(NO_3)_2$) and 0.75 M of thiourea. Ag/AgCl and graphite rod were used as reference and counter electrode, respectively. An electrodeposition process was then carried out at an applied potential of -1.0 V (*vs.* Ag/AgCl) for 100 s. Subsequently, the obtained sample of $Cu@Cu_2S@NiO_{1-x}S_x$ NWs (or $Cu@Cu_2S@CoO_{1-x}S_x$ NWs) on 3DF was cleaned with water three times followed by drying at 60 ^oC in a vacuum oven before it was investigated physicochemical and electrochemical properties.

Preparation of $Cu@NiCoO_2$ NWs network

For preparing $Cu@NiCoO_2$ NWs on 3DF, a working electrode based on a piece of the Cu NWs on 3DF (1 cm x 1 cm) was immersed in a 50 mL of aqueous solution containing 10 mM of $Ni(NO_3)_2$ and 10 mM $Co(NO_3)_2$. An electrodeposition step was then conducted at an applied potential of -1.0 V (*vs.* Ag/AgCl) for 100 s. After the reaction finished, the obtained sample of $Cu@NiCoO_2$ NWs on 3DF was washed by water three times and dried at 60 ^oC in a vacuum oven.

Turnover Frequency Calculations

Firstly, the ECSA was calculated according to C_{dl} value of materials [1]. In this research, metal foam was applied as substrate to support catalyst, thus its C_{dl} is much higher than that of a flat substrate having C_{dl} between 0.02-0.06 mF cm^{-2}. Therefore, the ECSA of materials could be assesses by following equation [2]:

$$A_{ECSA} = \frac{C_{dl\ (catalyst)}}{C_{dl(foam\ substrate)}}$$

where $C_{dl\ (foam\ substrate)}$ is around 1.7 mF cm^{-2} measured in 1.0 M KOH medium [2].

Therefore, A_{ECSA} of the Cu NWs (1.9 mF cm^{-2}), $Cu@NiCoO_2$ NWs (3.3 mF cm^{-2}), $Cu@Cu_2S@NiO_{1-x}S_x$ NWs (3.7 mF cm^{-2}), $Cu@Cu_2S@CoO_{1-x}S_x$ NWs (2.9 mF cm^{-2}), and

$Cu@Cu_2S@NiCoO_{2-x}S_x$ NWs (8.6 mF cm^{-2}) could be estimated to be 1.118, 1.941, 2.176, 1.706, and 5.059 cm^2.

We applied the following formula for evaluating the per site turnover frequency (TOF) [3,4]:

$$TOF = \frac{number\ of\ total\ hydrogen\ turn\ over/cm^2\ of\ geometric\ area}{number\ of\ active\ sites/cm^2\ of\ geometric\ area}$$

The total number of hydrogen turn overs was calculated from the current density according to:

$$no.\ of\ H_2 = (j\frac{mA}{cm^2})(\frac{1Cs^{-1}}{1000\ mA})(\frac{1\ mol\ e^-}{96485.3C})(\frac{1\ mol\ H_2}{2\ mol\ e^-})(\frac{6.023\times10^{23}H_2\ molecules}{1\ mol\ H_2}) = 3.12\times10^{15}\frac{H_2/s}{cm^2}\ per\ \frac{mA}{cm^2}$$

The number of active sites was evaluated from the roughness factor together with the unit cell, as seen in the case of Ni_5P_4 and $NiMoP_2$.[3] A same method was applied to evaluate TOF for our synthesized materials.

$$Active\ sites_{Cu} = (\frac{4\ atom/unit\ cell}{47.272Å^3/unit\ cell})^{\frac{2}{3}} = 1.927\times10^{15}\times atoms\ cm_{real}^{-2}$$

$$Active\ sites_{NiCoO_2} = (\frac{8\ atom/unit\ cell}{74.314Å^3/unit\ cell})^{\frac{2}{3}} = 2.263\times10^{15}\times atoms\ cm_{real}^{-2}$$

$$Active\ sites_{NiO_{1-x}S_x} = (\frac{4\ atom/unit\ cell}{72.9Å^3/unit\ cell})^{\frac{2}{3}} = 1.444\times10^{15}\times atoms\ cm_{real}^{-2}$$

$$Active\ sites_{CoO_{1-x}S_x} = (\frac{4\ atom/unit\ cell}{77.42Å^3/unit\ cell})^{\frac{2}{3}} = 1.387\times10^{15}\times atoms\ cm_{real}^{-2}$$

$$Active\ sites_{NiCoO_{2-x}S_x} = (\frac{8\ atom/unit\ cell}{74.314Å^3/unit\ cell})^{\frac{2}{3}} = 2.263\times10^{15}\times atoms\ cm_{real}^{-2}$$

Finally, TOF was can be calculated by an implied equation as following:

$$TOF = \frac{(3.12\times10^{15}\frac{H_2/s}{cm^2}\ per\ \frac{mA}{cm^2})|j|}{Active\ sites\times A_{ECSA}}$$

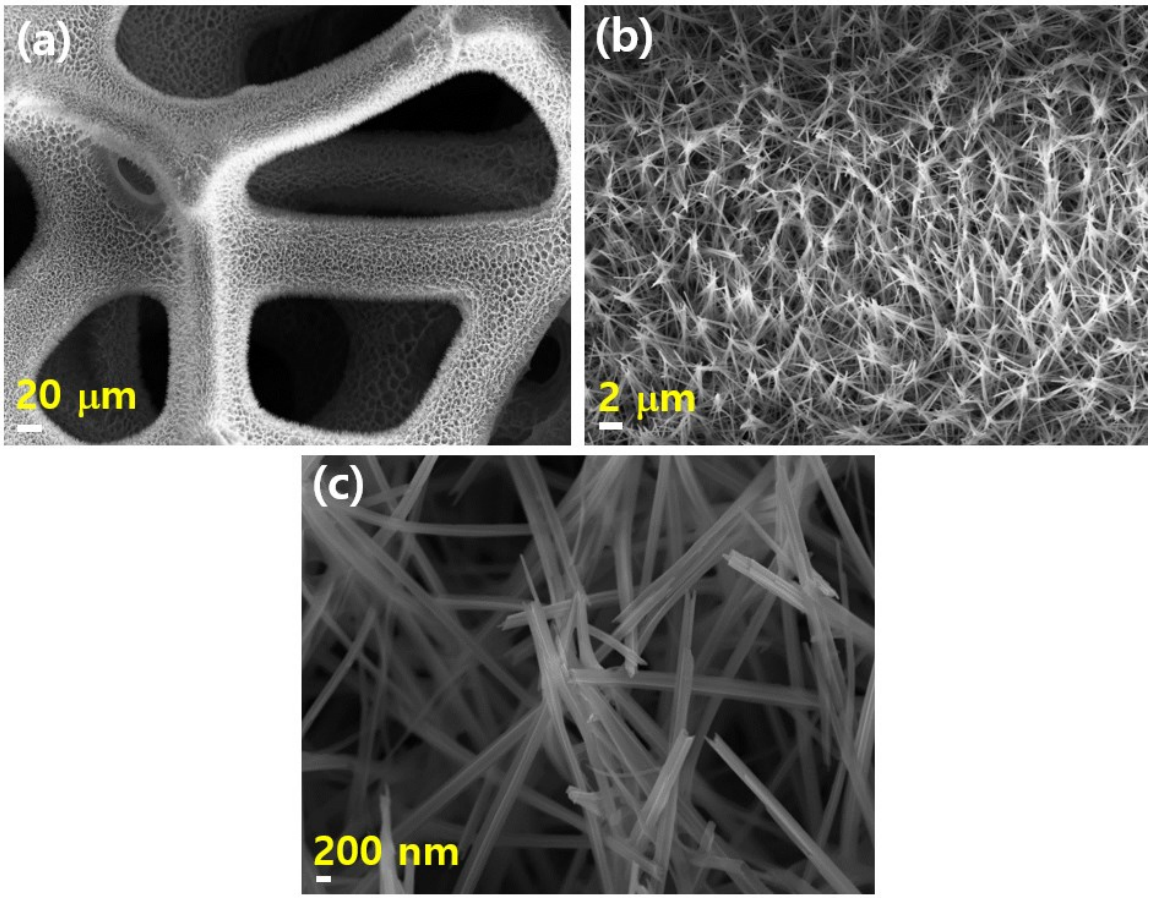

Figure S1. (a-c) SEM images at different magnifications of $Cu(OH)_2$ nanoneedles on 3DF.

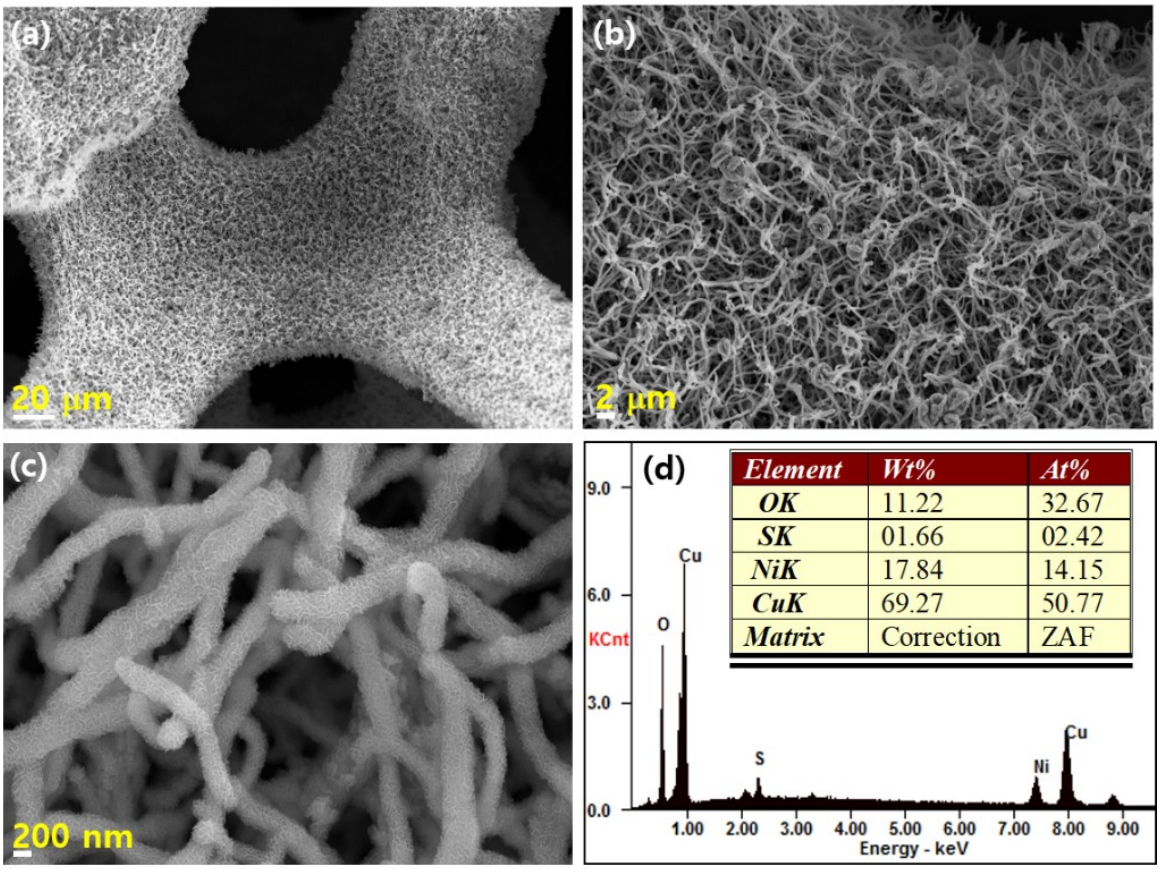

Figure S2. (a-c) SEM images and (d) EDAX spectrum of $Cu@Cu_2S@NiO_{1-x}S_x$ NWs on 3DF.

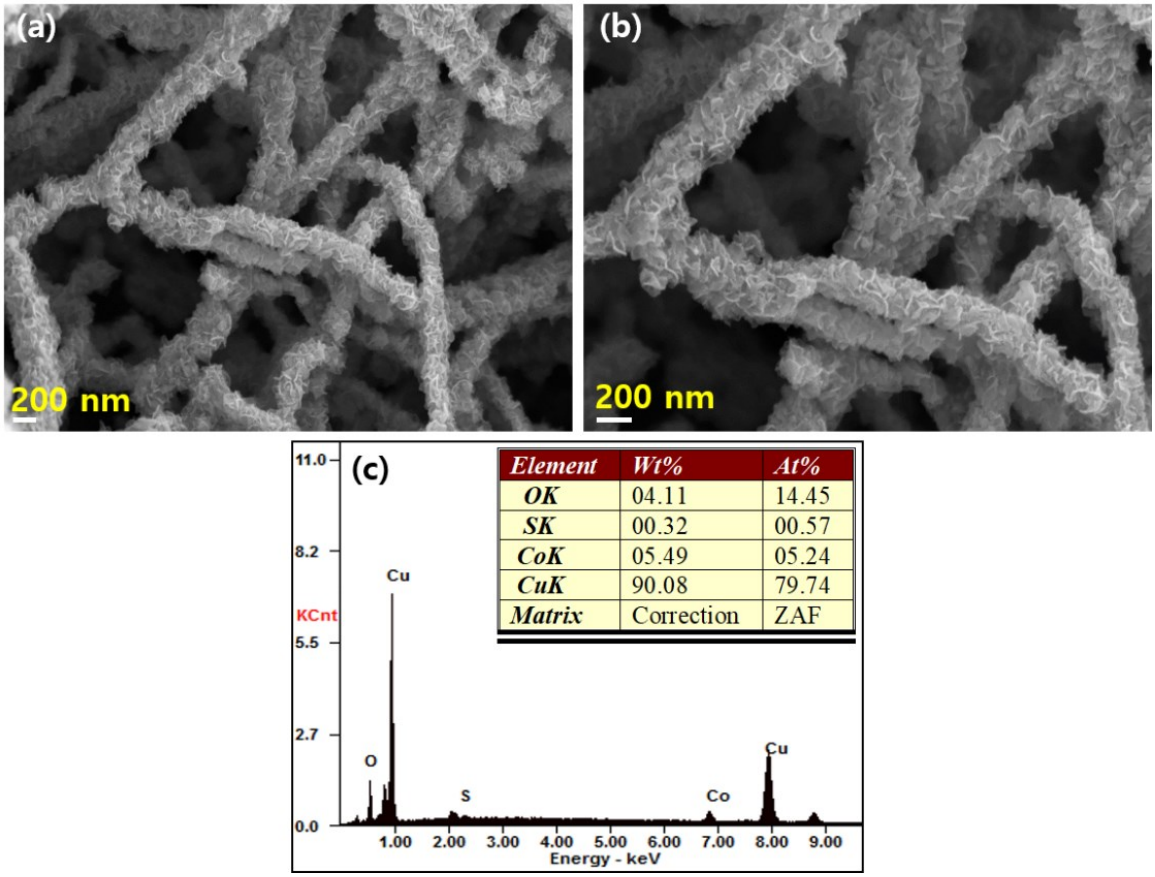

Figure S3. (a-b) SEM images and (c) EDAX spectrum of $Cu@Cu_2S@CoO_{1-x}S_x$ NWs on 3DF.

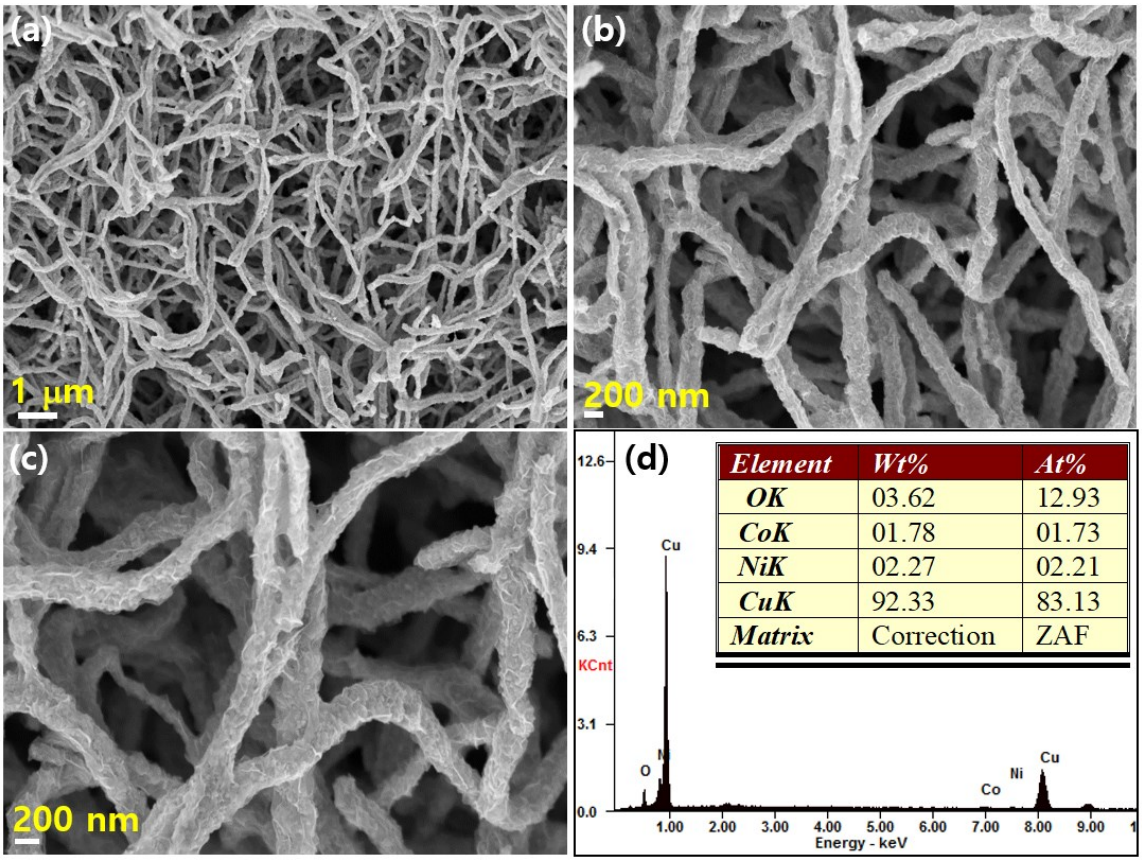

Figure S4. (a-c) SEM images and (d) EDAX spectrum of Cu@$NiCoO_2$ NWs on 3DF.

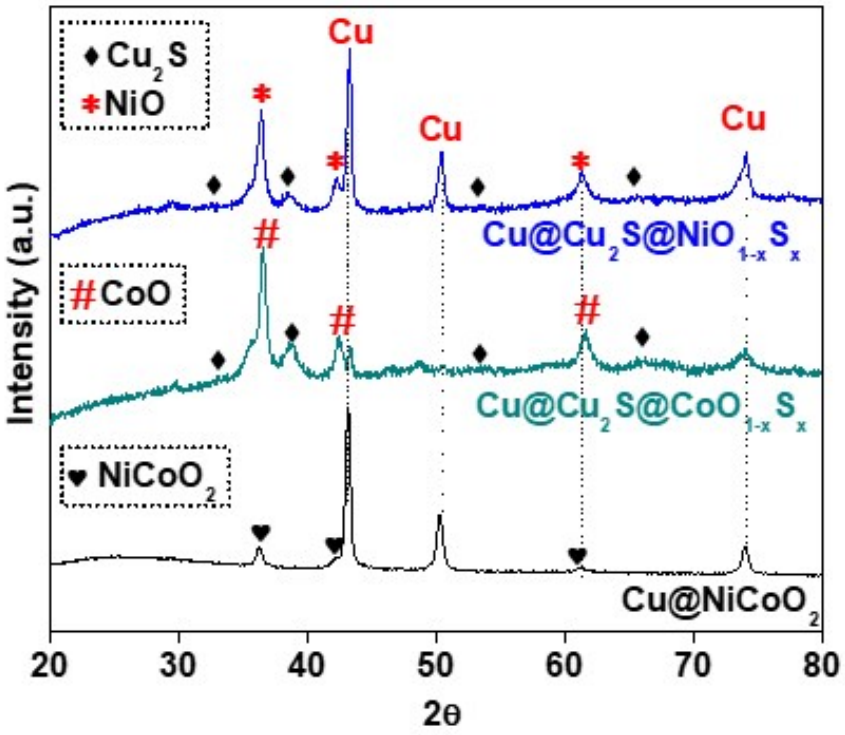

Figure S5. The crystalline structures of $Cu@NiCoO_2$ NWs, $Cu@Cu_2S@NiO_{1-x}S_x$ NWs, and $Cu@Cu_2S@CoO_{1-x}S_x$ NWs.

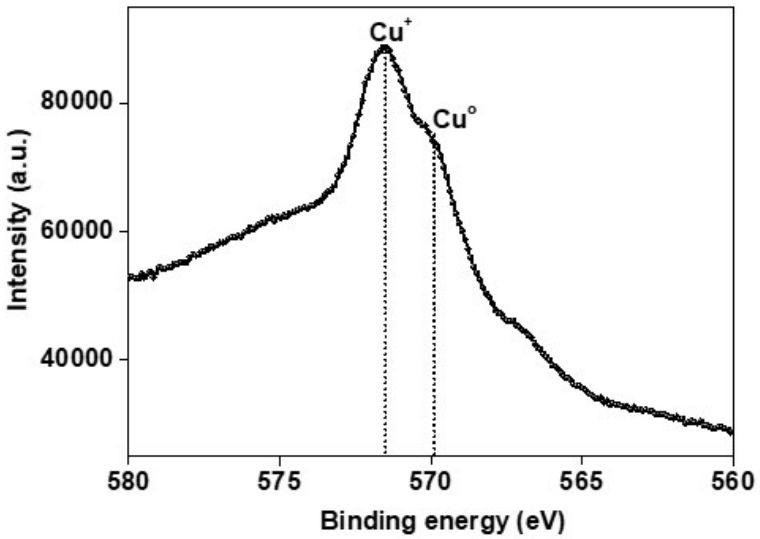

Figure S6. Cu(LMM) Auger spectrum of the Cu@Cu_2S@$NiCoO_{2-x}S_x$ NWs material.

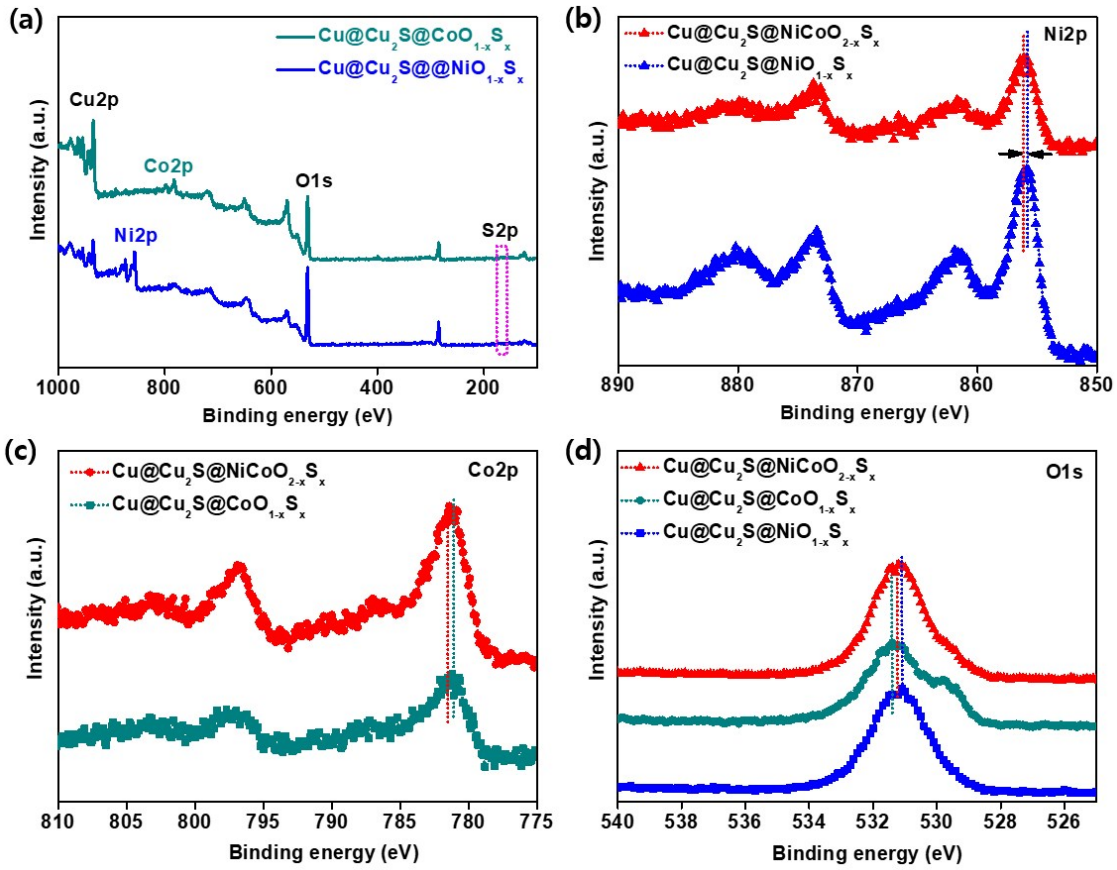

Figure S7. (a) Survey XPS spectra of $Cu@Cu_2S@NiO_{1-x}S_x$ NWs and $Cu@Cu_2S@CoO_{1-x}S_x$ NWs; (b) Comparison of Ni2p spectra between $Cu@Cu_2S@NiO_{1-x}S_x$ NWs and $Cu@Cu_2S@NiCoO_{2-x}S_x$ NWs; (c) Comparison of Co2p spectra between $Cu@Cu_2S@NiCoO_{2-x}S_x$ NWs and $Cu@Cu_2S@CoO_{1-x}S_x$ NWs; (d) Comparison of O1s spectra between $Cu@Cu_2S@NiCoO_{2-x}S_x$ NWs, $Cu@Cu_2S@CoO_{1-x}S_x$ NWs, and $Cu@Cu_2S@NiO_{1-x}S_x$ NWs.

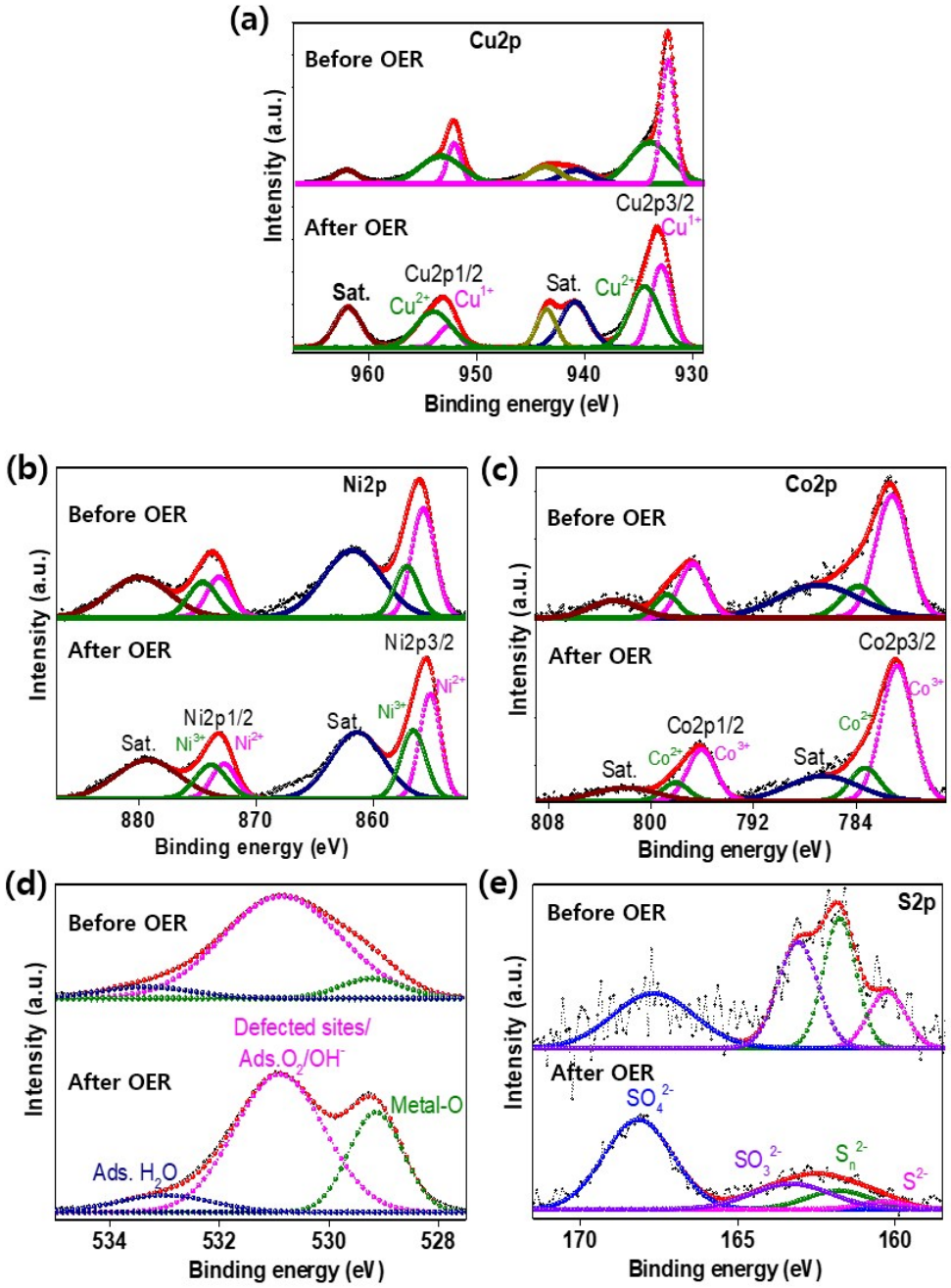

Figure S8. Comparison of (a) Cu2p, (b) Ni2p, (c)Co2p, (d) O1s, and (e) S2p XPS spectra of $Cu@Cu_2S@NiCoO_{2-x}S_x$ NWs before and after OER stability.

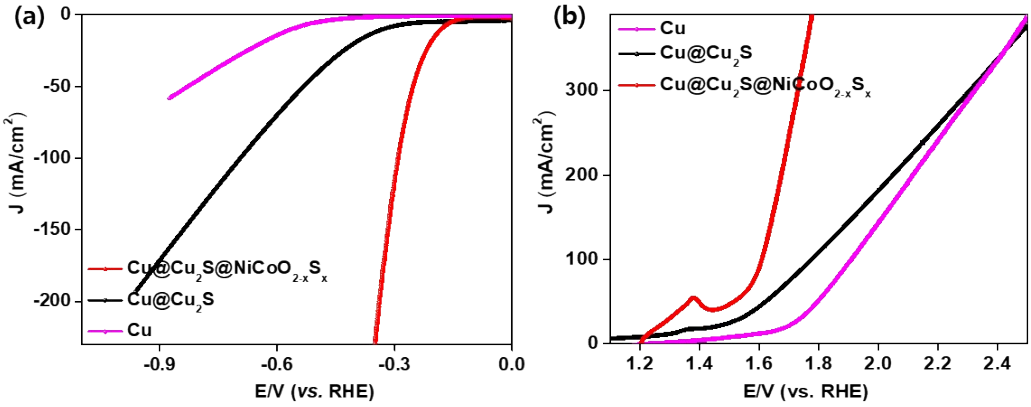

Figure S9. (a) HER and (b) OER performance of the Cu NWs, $Cu@Cu_2S$ NWs, $Cu@Cu_2S@NiCoO_{2-x}S_x$ NWs materials in 1.0 M KOH medium.

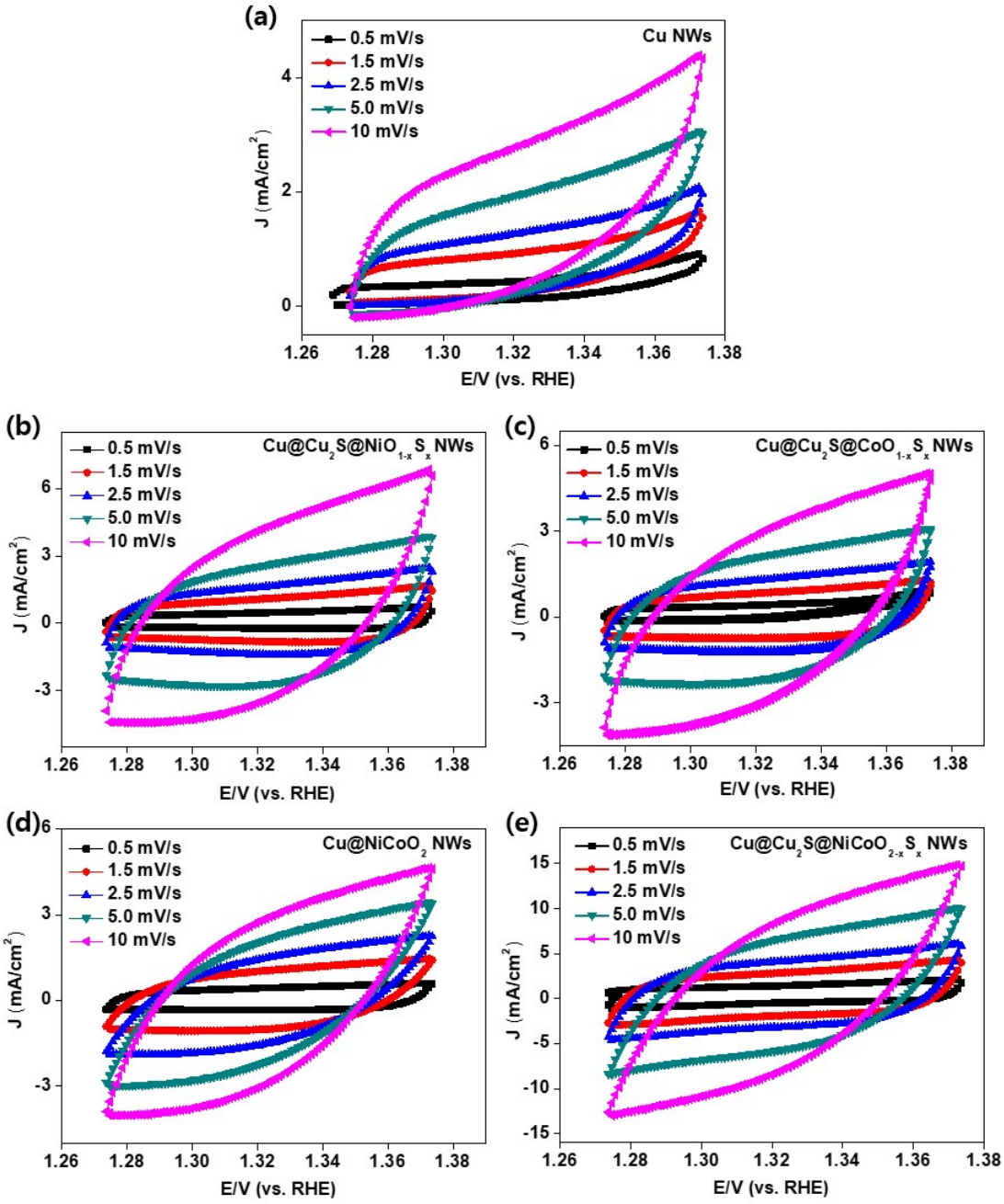

Figure S10. CV measurements in the potential range from 1.26 to 1.38 V (*vs.* RHE) at different scan rates: (a) Cu NWs, (b) $Cu@Cu_2S@NiO_{1-x}S_x$ NWs, (c) $Cu@Cu_2S@CoO_{1-x}S_x$ NWs, (d) $Cu@NiCoO_2$ NWs, and (e) $Cu@Cu_2S@NiCoO_{2-x}S_x$ NWs.

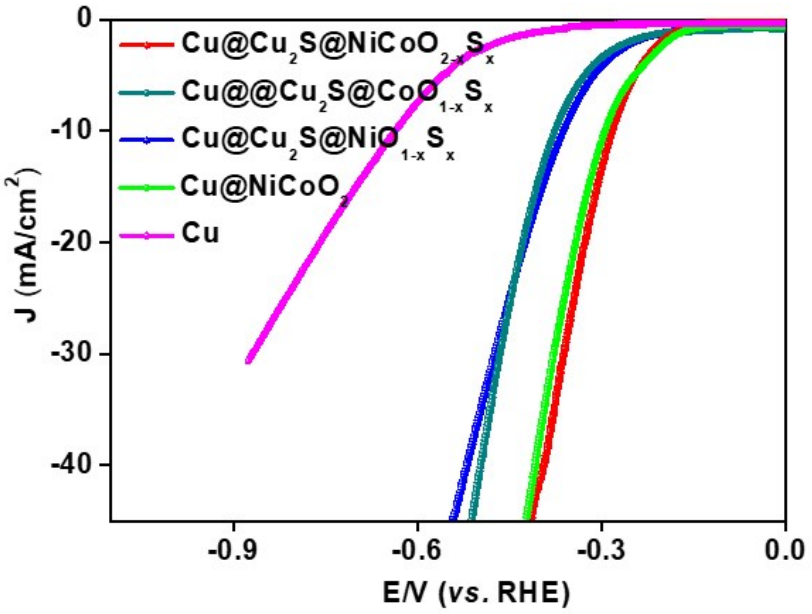

Figure S11. (C) LSV curves of materials towards HER normalized by the C_{dl} values.

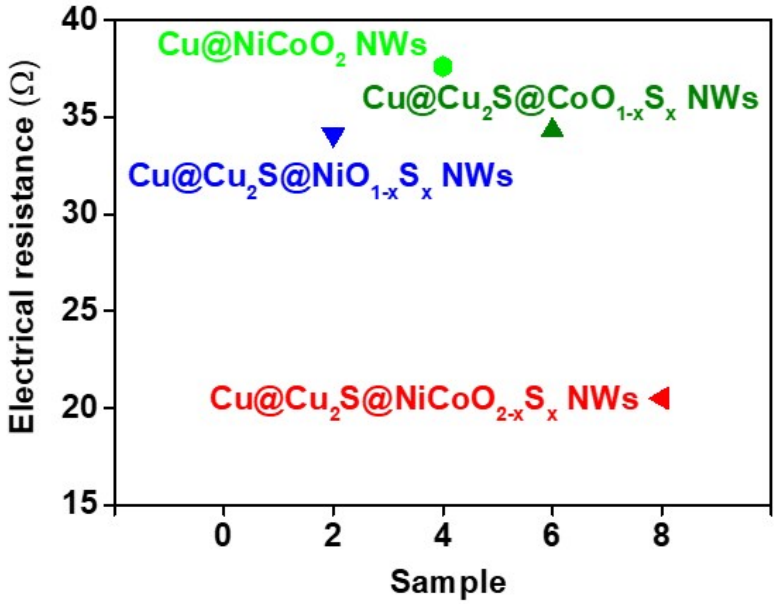

Figure S12. Electrical resistance of materials measured by 4-point probes method.

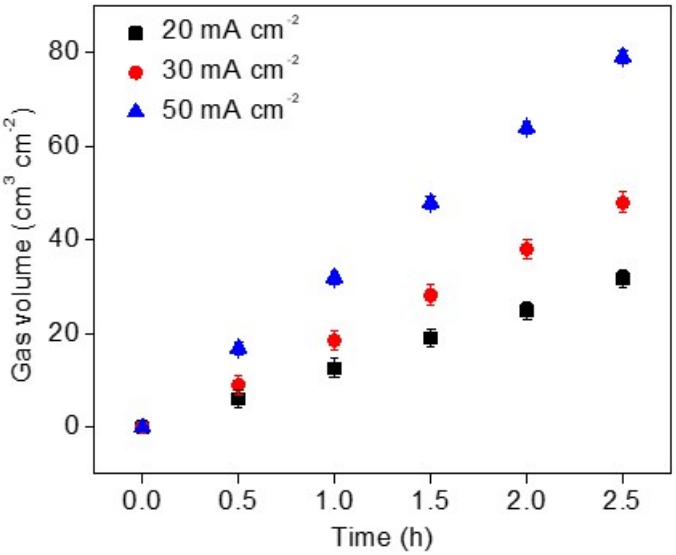

Figure S13. The evolution of total gas amount (H_2 + O_2) at different operating currents and time periods.

Table S1. Comparison of the Tafel slope between $Cu@Cu_2S@NiCoO_{2-x}S_x$ NWs catalyst with previous reports in 1.0 M KOH medium.

Electrocatalyst	Tafel slope (mV dec^{-1})	References
$Cu@Cu_2S@NiCoO_{2-x}S_x$ NWs	63	*This work*
$NiCo_2S_4$ NA/CC	141	*Nanoscale* **2015**, *7*, 15122
FeP NAs/CC	45	*ACS Catal*. **2014**, *4*, 4065.
CoOx@CN on GCE	115	*J. Am. Chem. Soc*. **2015**, *137*, 2688
PCPTF	53	*Adv. Mater.* **2015**, *27*, 3175.
CeO_2-Cu_3P/NF	132	*Nanoscale* **2018**, *10*, 2213.
Cu_3P/CF	63	*ACS Appl. Mater. Interfaces* **2016**, **8**, 23037
$Pr_{0.5}$BSCF	45	*Adv. Mater*. **2016**, *28*, 6442.
Co-NRCNTs	80	*Angew. Chem. Int. Ed.* **2014**, *53*, 4372.

Table S2. Comparison of the Tafel slope between $Cu@Cu_2S@NiCoO_{2-x}S_x$ catalyst with previous reports in 1.0 M KOH.

Electrocatalyst	**Tafel slope (mV dec^{-1})**	**References**
$Cu@Cu_2S@NiCoO_{2-x}S_x$ NWs /3DF	50	This work
Porous Ni-P nanoplates/GCE	64	*Energy Environ. Sci.* **2016**, *9*, 1246.
NiFe LDHNS@DG	52	*Adv. Mater.* **2017**, *29*, 1700017.
B,N:Mo_2C@BCN	61	*ACS Catal*. **2018**, *8*, 8296.
Fe-Ni_3C	62	*Angew. Chem. Int. Ed.* **2017**, *56*, 12566.
Ru-RuP_x-Co_xP	85	*Nano Energy* **2018**, *53,* 270.
CoS/CeO_x	50	*Angew. Chem. Int. Ed.* **2018**, *130*, 8790.
Coral-like Ni_3S_2 on Ni Foam	101	*ACS Appl. Mater. Interfaces* **2018**, *10*, 31330.

References

[1] C.C.L. McCrory, S. Jung, J.C. Peters, T.F. Jaramillo, *J. Am. Chem. Soc.* 2013, **135**, 16977–16987.

[2] H. Liang, A.N. Gandi, D.H. Anjum, X. Wang, U. Schwingenschlögl, H.N. Alshareef, *Nano Lett.,* 2016, **16**, 7718–7725.

[3] X.D. Wang, H.Y. Chen, Y.F. Xu, J.F. Liao, B.X. Chen, H.S. Rao, D. Bin Kuang, C.Y. Su, *J. Mater. Chem. A*., 2017, **5**, 7191–7199.

[4] J. Kibsgaard, T.F. Jaramillo, *Angew. Chemie-Int. Ed*., 2014, **53**, 14433–14437.